

# Structure Revision of Hassananes with Use of Quantum Mechanical $^{13}\text{C}$ NMR Chemical Shifts and UV–Vis Absorption Spectra

Jing Yang,<sup>†</sup> Sheng-Xiong Huang,<sup>\*,‡</sup> and Qin-Shi Zhao<sup>\*,‡</sup>

School of Chemistry and Chemical Technology, Shanghai Jiao Tong University, Shanghai, 200240, China, and State Key Laboratory of Phytochemistry and Plant Resources in West China, Kunming Institute of Botany, Chinese Academy of Sciences, Kunming, 650204, Yunnan, China

Received: August 13, 2008; Revised Manuscript Received: October 5, 2008

Geometry optimization and gauge including atomic orbitals (GIAO)  $^{13}\text{C}$  NMR chemical shifts in chloroform solvent calculated at the level of MPW1PW91/6-31G(d,p) were applied to przewalskins A (**3**) and B (**4**), which are novel diterpenoids with a 6/6/7 carbon ring skeleton. The good linear correlations between the calculated and experimental  $^{13}\text{C}$  NMR chemical shifts indicated the reliability of the computational method. This method was employed to the structural revision of natural product hassananes (**1**), which was reassigned to **2** with a similar skeleton as przewalskins A (**3**) and B (**4**). Furthermore, the UV–vis absorption spectra in gas phase and solvents were also predicted in order to further support our structure revision of hassananes.

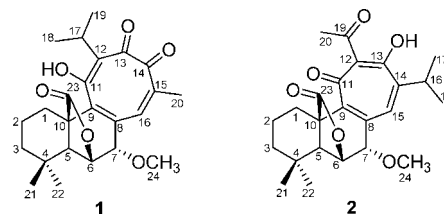
## 1. Introduction

The structural assignments of complex natural products by spectroscopic data, even with the rapid development of experimental NMR techniques, are still difficult and sometimes lead to erroneous and ambiguous conclusions. The recent application of the GIAO-DFT method to the calculation of the  $^{13}\text{C}$  NMR spectra<sup>1–6</sup> and time-dependent density functional theory (TD-DFT) to the calculation of CD<sup>7,8</sup> and UV<sup>9–12</sup> spectra have greatly facilitated the reliable determination of the natural products with novel structures.

Several papers were published on the structure validation and assignment of natural products by the calculations of GIAO  $^{13}\text{C}$  NMR chemical shifts. Barone et al. evaluated electron correlation contributions to the calculations of  $^{13}\text{C}$  NMR chemical shifts using the B3LYP method and extended the applicability of such a computational method to the interpretation of NMR spectra in apolar solutions.<sup>1</sup> The method was tested by studying three examples of revised structure assignments, analyzing how the theoretical  $^{13}\text{C}$  chemical shifts of both correct and incorrect structures matched the experimental data. Recently, Rychnovsky's report<sup>2</sup> optimized the geometries at the HF/3-21G level and obtained the GIAO-derived  $^{13}\text{C}$  NMR chemical shifts at the MPW1PW91/6-31G(d,p) level. In his work, the structure of the natural product hexacyclinol was reassigned from endoperoxide to diepoxide. This procedure gave a mean deviation  $|\Delta\delta|_{\text{mean}}$  of 6.8 ppm and a maximum deviation  $|\Delta\delta|_{\text{max}}$  of 22.0 ppm between theoretical and experimental  $^{13}\text{C}$  chemical shifts for the wrong structural assignment, but these improved to 1.8/5.8 ppm for the proposed right structure.

Time-dependent density functional theory allows an accurate prediction of the absorption spectra of organic compounds. The visible absorption spectra of several coumarin dyes were determined theoretically by Jacquemin et al. using the CIS and TD-DFT levels and compared to experimental values.<sup>11</sup> These calculations were performed in both gas phase and water. In

## SCHEME 1: Wrongly and Rightly Proposed Structures 1 and 2



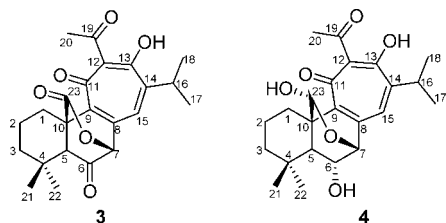
every case, the TD-DFT-PCM//DFT-PCM wavelengths were much closer to experimental data than those of CIS-PCM//HF-PCM. The electronic absorption spectra of luciferin and oxy-luciferin were also predicted by using both CIS and TD-DFT levels with a self-consistent isodensity polarized continuum model (SCI-PCM).<sup>12</sup> The calculated spectra using the TD-DFT method and the experimental absorption spectra in both the gas phase and aqueous solution were comparable to scaled CIS results.

Two different types of novel natural products, hassananes (**1**) and apiananes (**5**), were reported by Luis et al. in 1996 after isolation from the *Salvia apiana* Jeps collected in the coastal range and valleys of southern California.<sup>13a,b</sup> The structure of apiananes (**5**) was established without doubt by the X-ray experiment. The complicated structure **1** (Scheme 1) with a  $\text{C}_{23}$  new diterpenoid skeleton was proposed on the basis of the interpretation of spectroscopic data, especially NMR data. The authors proposed a biosynthetic pathway to account for the formation of **1** and **5** and supposed that hassananes (**1**) was derived biosynthetically from apiananes (**5**). Recently, two similar  $\text{C}_{23}$  diterpenoids, przewalskins A (**3**) and B (**4**) (Scheme 2), from the same genus *Salvia przewalskii* Maxim, were reported by our group. We reasonably explained the biosynthetic origin of przewalskin B (**4**) from a normal *o*-quinone.<sup>14</sup> Careful chemical structural inspections among hassananes (**1**), przewalskin B (**4**), and apiananes (**5**) revealed that hassananes (**1**) might have the wrong structure assignment and structure **1** should be revised to **2**. From a biogenetic view, hassananes (**2**) was not biosynthetically derived from apiananes (**5**). On the

\* Corresponding authors. S.-X.H., Q.-S.Z.: phone (86) 871-5223058, fax (86) 871-5215783, e-mail sxhuang80@yahoo.com and qinshizhao@yaho.com.

<sup>†</sup> Shanghai Jiao Tong University.

<sup>‡</sup> Chinese Academy of Sciences.

**SCHEME 2: Chemical Structures of Przewalskins A (3) and B (4)**


contrary, hassananes (**2**) was the precursor of **5**. One possible pathway for the formation of **5** is illustrated in Scheme 3. The double bond between C-14 and C-15 first underwent reduction to generate the 14,15-dihydrohassananes (**2a**), followed by the aldol reaction leading to the formation of the C11–C14 bond and the cleavage of the C11–C12 bond. The last step was the five-membered ring closure by an intramolecular aldol condensation. Interest in these findings triggered us to reexamine the original structural assignment of hassananes (**1**). Our aim is to provide valid computational support to structural revision of natural product hassananes (**1**), which is reassigned to **2** (in Scheme 1). Przewalskins A (**3**) and B (**4**) are used to evaluate the different combinations of methods to determine whether they will be applicable to the hassananes case. We initially select przewalskins A (**3**) and B (**4**) to evaluate the computational methods since not only do they have similar skeletons with **2**, but each molecule also is relatively rigid and they are largely free of conformational ambiguities. Two computational tools acted as the evaluation standards. First, the experimental  $^{13}\text{C}$  NMR chemical shifts are compared with those predicted by GIAO-derived  $^{13}\text{C}$  chemical shift calculations. Second, the TD-DFT methods are applied to predict the absorption spectra based upon the geometries optimized at the DFT levels of theory. The solvent effect is also considered in the calculations.

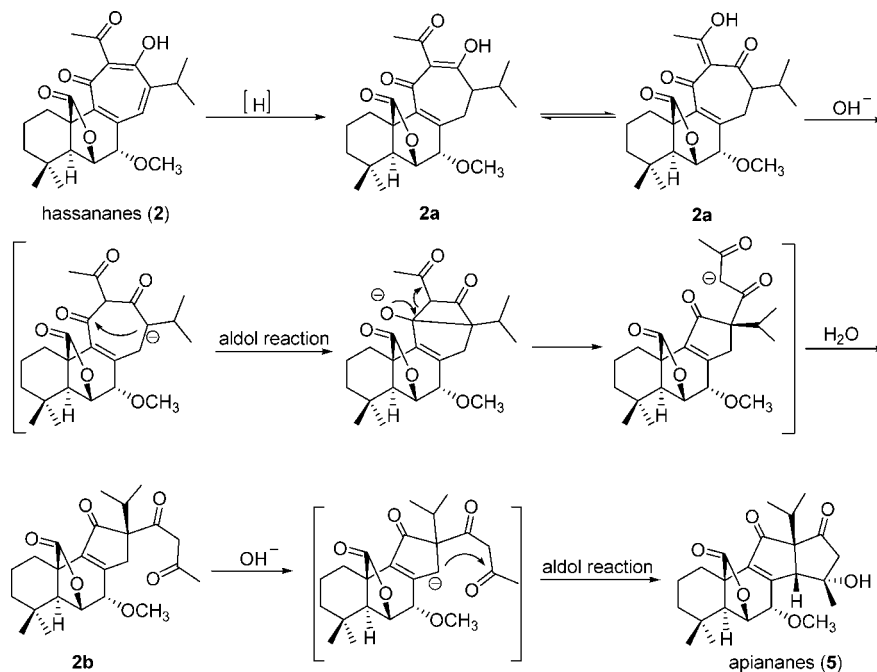
**2. Computational Methods**

First, for the calculations of  $^{13}\text{C}$  NMR chemical shifts, HF/3-21G, B3LYP $^{15}$ /6-31G(d), and MPW1PW91 $^{16}$ /6-31G(d,p) meth-

ods were used to optimize the structures. For all optimized structures, vibrational spectra were calculated to ensure that no imaginary frequencies for energy minimum were obtained. NMR calculations were performed at the levels of B3LYP/6-311+G(2d,p), MPW1PW91/6-31G(d,p), MPW1PW91/6-31+G(d,p), MPW1PW91/6-31+G(2d,p), and MPW1PW91/6-31++G(2d,p) with the gauge-independent atomic orbital (GIAO) method. $^{17-19}$  The solvent effect was considered by using chloroform in the calculations to resemble the experimental condition. The polarized continuum model (PCM) of Tomasi et al. was used. $^{20-22}$

The calculated  $^{13}\text{C}$  NMR chemical shifts were analyzed by subtracting the isotopic shifts for TMS calculated with the same methods. $^{23-25}$  Different conformers for structures **1–4** were considered. The  $^{13}\text{C}$  NMR chemical shifts in each compound were considered as the average values of the same atoms in the different conformers. The average values were obtained by the Boltzmann distributions, using the relative Gibbs free energies as weighting factors. The differences  $\Delta\delta$  were determined by subtracting the experimental chemical shifts  $\delta_{\text{exp}}$  from the scaled calculated chemical shifts  $\delta_{\text{scal,calc}}$ . The linear correlations between scaled calculated and experimental chemical shifts and functional expressions were employed. The scaled calculated  $^{13}\text{C}$  NMR chemical shifts were obtained from the following:  $\delta_{\text{scal,calc}} = (\delta_{\text{calc}} - \text{intercept})/\text{slope}$ , where the intercept and the slope are the least-squares parameters obtained by the linear fit lines between the experimental and calculated chemical shifts. $^1$

Second, for the calculations of the absorption spectra, the ground state geometries were obtained from optimization with B3LYP/6-31G(d) and MPW1PW91/6-31G(d,p) methods. The absorption wavelengths were predicted by using the same TD-DFT methods $^{26-29}$  on the basis of optimized ground state geometries. Solvent effect was also considered by using PCM model. The PCM model takes account of specific molecular shape in the construction of the solute cavity. The solvents chosen in our calculations were methanol and ethanol. The oscillator strengths are very helpful in assigning the calculated

**SCHEME 3: Proposed Formation of Apiananes (5) from Hassananes (2)**


**TABLE 1: Calculated Chemical Shifts (ppm) for Przewalskin A (3)**

carbon no.	A <sup>a</sup>	B <sup>b</sup>	C <sup>c</sup>	D <sup>d</sup>	E <sup>e</sup>	F <sup>f</sup>	G <sup>g</sup>	exptl <sup>h</sup>
C-1	29.9	32.9	30.6	30.6	31.2	30.8	30.6	26.0
C-2	19.8	22.3	20.4	20.5	21.2	21.4	21.5	18.2
C-3	40.3	45.1	41.4	40.8	42.3	41.8	41.9	40.6
C-4	39.8	45.2	38.7	39.2	40.7	39.0	39.9	36.1
C-5	52.4	58.1	52.6	52.9	55.5	54.4	55.1	51.7
C-6	198.2	212.7	198.6	201.1	203.2	203.2	202.6	200.6
C-7	83.4	91.9	84.5	84.4	86.3	85.1	85.5	83.9
C-8	129.5	142.7	131.8	133.2	135.3	134.1	133.9	134.7
C-9	145.9	161.0	149.9	149.3	150.1	148.2	148.7	146.0
C-10	52.8	58.5	53.7	54.2	55.8	53.8	53.7	50.5
C-11	180.6	191.5	180.3	181.6	182.7	183.4	183.3	186.3
C-12	118.5	127.7	120.6	121.0	122.1	120.1	121.0	120.6
C-13	166.4	182.0	171.2	172.1	173.0	170.5	172.4	174.3
C-14	147.2	161.6	149.7	151.1	153.9	151.5	152.3	151.8
C-15	121.3	134.3	126.9	127.9	129.4	129.1	128.7	127.0
C-16	33.3	35.8	32.6	33.1	35.2	34.6	35.45	30.5
C-17	19.1	21.2	21.0	20.9	19.8	20.2	20.8	22.5
C-18	22.9	24.7	23.8	23.8	25.3	24.9	24.2	22.5
C-19	198.8	215.4	200.8	201.8	203.1	203.1	203.4	204.1
C-20	30.1	32.6	30.7	31.2	33.0	32.8	32.6	28.6
C-21	19.7	21.1	21.2	21.6	21.3	20.5	20.8	20.1
C-22	31.6	34.2	33.1	32.8	33.6	32.4	32.6	33.2
C-23	163.1	177.8	163.7	166.8	169.0	171.3	170.3	170.5
$ \Delta\delta _{\max}$	7.9	12.1	6.8	4.7	5.3	4.8	5.0	
$ \Delta\delta _{\text{mean}}$	3.0	6.6	2.3	2.0	2.7	2.2	2.1	

<sup>a</sup> The chemical shifts were computed at the MPW1PW91/6-31G(d,p) level of theory, using the HF/3-21G-optimized geometries. <sup>b</sup> The chemical shifts were computed at the B3LYP/6-311+G(2d,p) level of theory, using the B3LYP/6-31G(d)-optimized geometries. <sup>c</sup> The chemical shifts were computed at the MPW1PW91/6-31G(d,p) level of theory, using the MPW1PW91/6-31G(d,p)-optimized geometries. <sup>d</sup> The chemical shifts were computed at the MPW1PW91/6-31G(d,p) level of theory in the chloroform solvent, using the MPW1PW91/6-31G(d,p)-optimized geometries. <sup>e</sup> The chemical shifts were computed at the MPW1PW91/6-31+G(d,p) level of theory in the chloroform solvent, using the MPW1PW91/6-31G(d,p)-optimized geometries. <sup>f</sup> The chemical shifts were computed at the MPW1PW91/6-31+G(2d,p) level of theory in the chloroform solvent, using the MPW1PW91/6-31G(d,p)-optimized geometries. <sup>g</sup> The chemical shifts were computed at the MPW1PW91/6-31++G(2d,p) level of theory in the chloroform solvent, using the MPW1PW91/6-31G(d,p)-optimized geometries. <sup>h</sup> From ref 14.

electronic spectra to experimental absorption. Therefore, the oscillator strengths, *f*, were calculated by using TD-DFT methods.

All calculations were carried out with the Gaussian 03 program package.<sup>30</sup>

### 3. Results and Discussion

**3.1. <sup>13</sup>C NMR Chemical Shifts.** First, przewalskin A (3) is used to validate the computational methods. The crystal structure<sup>9</sup> acted as the initial optimized structure of przewalskin A (3), which corresponds to the minimum energy conformer. The calculated <sup>13</sup>C NMR chemical shifts for przewalskin A (3) with different combined methods can be seen in Table 1. The calculations using methods A, B, and C are in the gas phase. From the maximum differences ( $|\Delta\delta|_{\max}$ ) and the average differences ( $|\Delta\delta|_{\text{mean}}$ ) between the calculated and experimental chemical shifts, method C (MPW1PW91/6-31G(d,p)-optimized geometry followed by MPW1PW91/6-31G(d,p) <sup>13</sup>C NMR calculation) gives the best results among the three methods whose corresponding values are 6.8 and 2.3 ppm, respectively.

**TABLE 2: Calculated Chemical Shifts (ppm) for Przewalskin B (4)**

carbon no.	A <sup>a</sup>	B <sup>b</sup>	C <sup>c</sup>	D <sup>d</sup>	exptl <sup>e</sup>
C-1	32.2	34.1	32.9	33.1	27.8
C-2	20.8	21.0	21.5	21.6	18.8
C-3	41.0	42.3	42.4	41.7	41.7
C-4	35.8	37.2	35.3	35.7	34.3
C-5	53.0	55.6	53.8	53.4	55.4
C-6	70.6	71.4	70.0	70.7	70.1
C-7	76.2	77.0	76.7	76.3	75.3
C-8	137.2	139.1	137.5	137.5	138.8
C-9	151.6	151.6	149.9	150.1	147.9
C-10	50.8	51.8	50.6	50.5	48.3
C-11	185.2	184.7	184.8	184.9	189.7
C-12	121.2	122.7	120.4	121.4	120.9
C-13	171.1	172.0	171.1	171.1	173.7
C-14	144.8	147.8	145.9	145.9	146.2
C-15	132.7	134.4	134.0	134.3	133.4
C-16	32.1	35.2	34.3	35.2	30.5
C-17	21.3	20.5	20.6	21.2	22.7
C-18	24.0	25.5	24.9	24.4	22.9
C-19	202.0	203.4	203.4	203.6	205.5
C-20	31.3	33.1	32.3	32.8	28.5
C-21	24.5	24.3	23.3	23.1	23.2
C-22	34.2	35.5	34.5	34.6	34.0
C-23	91.2	92.3	92.2	92.2	90.9
$ \Delta\delta _{\max}$	4.5	6.3	5.1	5.3	
$ \Delta\delta _{\text{mean}}$	1.8	2.2	1.8	1.8	

<sup>a</sup> The chemical shifts were computed at the MPW1PW91/6-31G(d,p) level of theory in the chloroform solvent, using the MPW1PW91/6-31G(d,p)-optimized geometries. <sup>b</sup> The chemical shifts were computed at the MPW1PW91/6-31+G(d,p) level of theory in the chloroform solvent, using the MPW1PW91/6-31G(d,p)-optimized geometries. <sup>c</sup> The chemical shifts were computed at the MPW1PW91/6-31+G(2d,p) level of theory in the chloroform solvent, using the MPW1PW91/6-31G(d,p)-optimized geometries. <sup>d</sup> The chemical shifts were computed at the MPW1PW91/6-31++G(2d,p) level of theory in the chloroform solvent, using the MPW1PW91/6-31G(d,p)-optimized geometries. <sup>e</sup> From ref 14.

After a self-consistent reaction field correction in chloroform solvent (method D) on the basis of method C, the difference improves to 4.7 and 2.0 ppm, respectively. We further test the effect of different basis sets using the MPW1PW91 method in chloroform solvent (methods E–G). From the maximum differences and the average differences, it can be seen that the 6-31G(d,p) basis set is enough to give the best <sup>13</sup>C NMR chemical shifts contrasted with other larger basis sets. To sum up, it can be concluded that method D, i.e. MPW1PW91/6-31G(d,p)-PCM//MPW1PW91/6-31G(d,p), can give results which are the most similar with the experimental results for przewalskin A (3).

Second, przewalskin B (4) is also used to evaluate the different computational methods. The calculated <sup>13</sup>C NMR chemical shifts for przewalskin B (4) with different combined methods can be seen in Table 2. In all tests, the minimum energy conformer is considered. The MPW1PW91/6-31G(d,p) method is used to optimize the structure. MPW1PW91 functionals with various basis sets including 6-31G(d,p), 6-31+G(d,p), 6-31+G(2d,p), and 6-31++G(2d,p) are used to calculate the <sup>13</sup>C NMR chemical shifts considering the solvent effect in chloroform. The same is true with przewalskin A (3), where the MPW1PW91/6-31G(d,p)-PCM//MPW1PW91/6-31G(d,p) method (method A) can also give the best results among the four methods for przewalskin B (4). The average chemical shift difference ( $|\Delta\delta|_{\text{mean}}$ ) for przewalskin B (4) is 1.8 ppm, and the maximum difference ( $|\Delta\delta|_{\max}$ ) is 4.5 ppm.

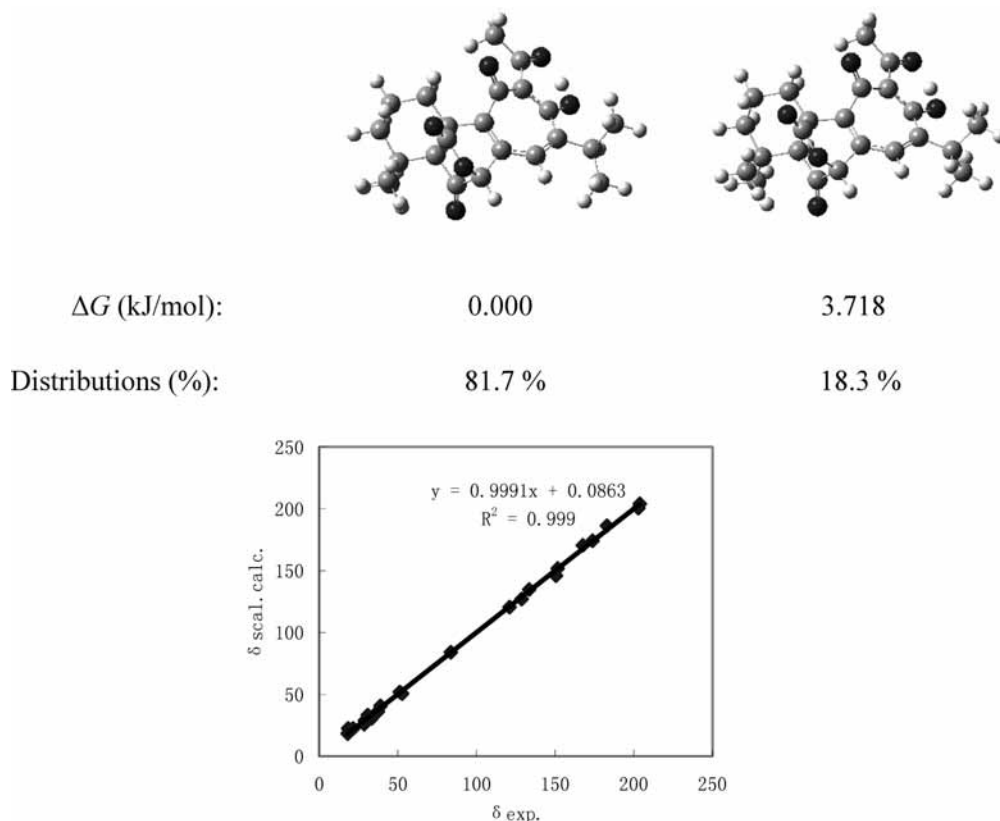


**Figure 1.** Structures and linear correlation between the scaled calculated (at the level of MPW1PW91/6-31G(d,p)-PCM//MPW1PW91/6-31G(d,p)) and experimental  $^{13}\text{C}$  NMR chemical shifts for przewalskin A (3).

Finally, we consider the effect of the different conformations for przewalskins A (3) and B (4). Figure 1 describes the geometrical structures of the two conformers for przewalskin A (3). In the left and right conformers the torsion angles of C15–C14–C16–H16 are  $132.2^\circ$  and  $-13.1^\circ$ , respectively, with Boltzmann distributions equal to 81.7% and 18.3%, respectively. In the same way, the geometrical structures of the two conformers for przewalskin B (4) are also shown in Figure 2. In the left and right conformers the torsion angles of C15–C14–C16–H16 are  $132.0^\circ$  and  $-12.7^\circ$ , respectively, with Boltzmann distributions equal to 83.9% and 16.1%, respectively. The scaled calculated GIAO  $^{13}\text{C}$  NMR chemical shifts for the optimized przewalskins A (3) and B (4) are plotted against the corresponding experimental  $^{13}\text{C}$  NMR chemical shifts. The linear correlations of the chemical shifts are shown in Figures 1 and 2. For both structures, the least-squared parameters for intercept, slope, and the square of correlation coefficient ( $R^2$ ) are reported in the figures. Calculated from  $R^2$ ,  $R$  values are equal to 0.9995 and 0.9994 for przewalskins A (3) and B (4), respectively. The correlations are very good, which supports this method to evaluate the natural products, przewalskins A (3) and B (4).

Therefore in the following calculations, the MPW1PW91/6-31G(d,p)-PCM//MPW1PW91/6-31G(d,p) method is chosen to reassign structure 1 to 2.

The reported structure of hassananes (1) is evaluated by using the above  $^{13}\text{C}$  chemical shift method, and the scaled calculated  $^{13}\text{C}$  NMR chemical shift results are listed in Table 3. For the compound, two conformers are considered. The structures of the two conformers can be seen in Figure 3. In the left structure the torsion angle of C11–C12–C17–H17 is  $-12.0^\circ$  and in the right structure the torsion angle of C11–C12–C17–H17 is

$176.7^\circ$ . Their Boltzmann distributions are equal to 91.3% and 8.7%, respectively. Atoms C-13, C-15, and C-16 show deviations of more than 10 ppm. On the other hand, from the values of the maximum deviation  $|\Delta\delta|_{\text{max}}$  and the average deviation  $|\Delta\delta|_{\text{mean}}$ , we can see that the scaled calculated  $^{13}\text{C}$  NMR chemical shifts are better than no scaled ones. The average deviation  $|\Delta\delta_{(\text{scal. calc.} - \text{exp.})}|_{\text{mean}}$  is 4.96 ppm and the maximum deviation  $|\Delta\delta_{(\text{scal. calc.} - \text{exp.})}|_{\text{max}}$  is 34.01 ppm. Considering the excellent performance of the predictive results on similar natural products przewalskins A (3) and B (4) in Tables 1 and 2, it can be concluded that the proposed structure 1 is incorrect. Therefore in the following discussion, structure 2 will be examined.

Analogously, the theoretical  $^{13}\text{C}$  NMR chemical shift values calculated for 2 are listed in Table 4 and the analysis of 2 resulted in the chemical shift differences  $\Delta\delta$  between the theoretical and experimental chemical shifts. Two conformers are also considered. The geometrical structures of the two conformers can be seen in Figure 4. In the left structure the torsion angle of C15–C14–C16–H16 is  $-47.6^\circ$  and in right structure the torsion angle of C15–C14–C16–H16 is  $169.1^\circ$ . Their Boltzmann distributions are equal to 71.2% and 28.8%, respectively. We also consider the rotation of the torsion angle C11–C12–C19–O19. As shown in Figure 4 there is a hydrogen bond between the oxygen atom in the carbonyl group C19=O and the hydrogen atom in the hydroxyl group C13–OH. So the rotation of the torsion angle C11–C12–C19–O19 needs to consume high energy (largely above 11 kJ/mol), and the Boltzmann distribution is nearly zero. Seen from Table 4, it also can be concluded that the scaled calculated  $^{13}\text{C}$  NMR chemical shifts are more accurate than no scaled ones contracted with the maximum deviation  $|\Delta\delta|_{\text{max}}$  and the average deviation  $|\Delta\delta|_{\text{mean}}$ . The calculations with the MPW1PW91/6-31G(d,p)-PCM//MPW1PW91/6-31G(d,p) method result in relatively small



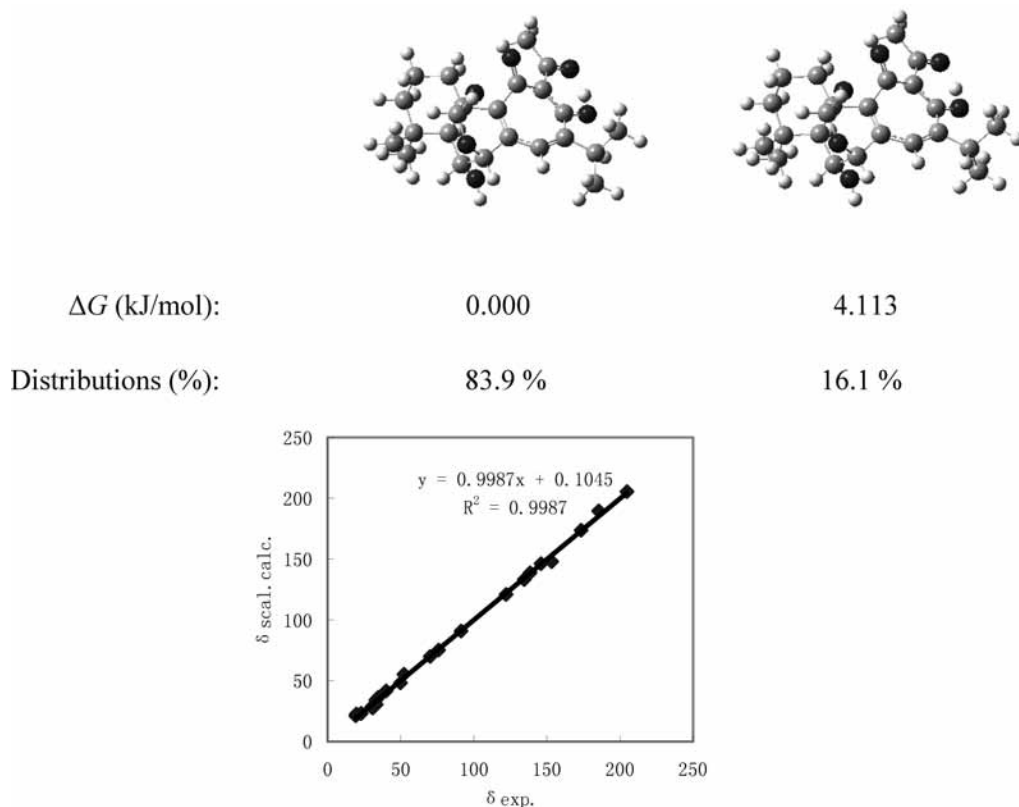


**Figure 2.** Structures and linear correlation between the scaled calculated (at the level of MPW1PW91/6-31G(d,p)-PCM//MPW1PW91/6-31G(d,p)) and experimental  $^{13}\text{C}$  NMR chemical shifts for przewalskin B (**4**).

**TABLE 3: Differences between the Calculated<sup>a</sup> and Experimental  $^{13}\text{C}$  NMR Chemical Shifts for the Wrongly Proposed Structure 1**

carbon no.	$\delta_{\text{calc.}}$	$\delta_{\text{scal. calc.}}$	$\delta_{\text{exp.}}^b$	$\Delta\delta_{(\text{calc.}-\text{exp.})}$	$\Delta\delta_{(\text{scal. calc.}-\text{exp.})}$
C-1	27.41	26.25	26.40	1.01	-0.15
C-2	20.66	19.08	18.60	2.06	0.48
C-3	38.65	38.19	38.14	0.51	0.05
C-4	33.05	32.24	22.34	10.71	9.90
C-5	50.09	50.34	50.18	-0.09	0.16
C-6	71.61	73.20	73.02	-1.41	0.18
C-7	77.19	79.12	79.45	-2.26	-0.33
C-8	131.05	136.32	132.07	-1.02	4.25
C-9	137.15	142.80	146.62	-9.47	-3.82
C-10	50.06	50.31	45.83	4.23	4.48
C-11	141.99	147.95	149.08	-7.09	-1.13
C-12	120.00	124.59	119.82	0.18	4.77
C-13	200.52	210.12	189.11	11.41	21.01
C-14	192.86	201.98	203.12	-10.26	-1.14
C-15	135.83	141.40	175.41	-39.58	-34.01
C-16	137.39	143.06	132.00	5.39	11.06
C-17	31.40	30.49	30.20	1.2	0.29
C-18	23.38	21.97	22.76	0.62	-0.79
C-19	21.48	19.95	21.88	-0.4	-1.93
C-20	22.69	21.24	28.08	-5.39	-6.84
C-21	24.03	22.66	31.34	-7.31	-8.68
C-22	32.33	31.48	31.34	0.99	0.14
C-23	170.76	178.51	175.71	-4.95	2.80
C-24	57.80	58.52	59.19	-1.39	-0.67
$ \Delta\delta _{\text{max}}$				39.58	34.01
$ \Delta\delta _{\text{mean}}$				5.37	4.96

<sup>a</sup> The chemical shifts were computed at the MPW1PW91/6-31G(d,p) level of theory in the chloroform solvent, using the MPW1PW91/6-31G(d,p)-optimized geometries. <sup>b</sup> From ref 13a.

$\Delta\delta_{(\text{scal. calc.}-\text{exp.})}$  values, and the average chemical shift difference is 1.59 ppm. The largest deviations are observed for C-9 and

C-17 which are 4.93 and  $-4.21$  ppm, respectively. The calculated  $^{13}\text{C}$  NMR chemical shifts agree well with the experimental chemical shifts. Therefore, we propose that the correct structure is **2**.

The scaled calculated GIAO  $^{13}\text{C}$  NMR chemical shifts for the optimized structures **1** and **2** are plotted against the corresponding experimental  $^{13}\text{C}$  NMR chemical shifts. The linear correlations of the chemical shifts are shown in Figures 3 and 4. For both structures, the values for intercept, slope, and the square of correlation coefficient ( $R^2$ ) are reported in the figures. Calculated from  $R^2$ ,  $R$  values are equal to 0.9891 and 0.9995 for **1** and **2**, respectively. The  $R$  value for **1** (0.9891) is much lower than that calculated for **2** (0.9995). Literature data show that for a corrected structure, the  $R$  value is usually greater than or equal to 0.995.<sup>1</sup> The correlation is very poor for **1**, but the calculated  $^{13}\text{C}$  chemical shifts predicted for **2** correlate very well with those reported in the experiment. Therefore, our results strongly suggest that the rightly proposed structure is **2** rather than **1**.

**3.2. UV-Vis Absorption Spectra.** In Tables 5 and 6, the calculated absorption spectra  $\lambda$  and oscillator strengths  $f$  obtained are listed at the TD-DFT level of theory based on the DFT-optimized geometries in the gas phase and solutions for przewalskins A (**3**) and B (**4**), structures **1** and **2**, respectively. The experimental values are also included in the tables for comparison. Though the ten singlet-singlet spin-allowed excited states are taken into account in the calculations by using the TD-DFT methods, we only present the absorption spectra whose oscillator strengths are relatively big.

In the TD-DFT calculations, two methods, i.e. B3LYP/6-31G(d) and MPW1PW91/6-31G(d,p), are used. Compared to the level of B3LYP/6-31G(d), MPW1PW91/6-31G(d,p) have been shown to yield more accurate theoretical results agreeing well with the

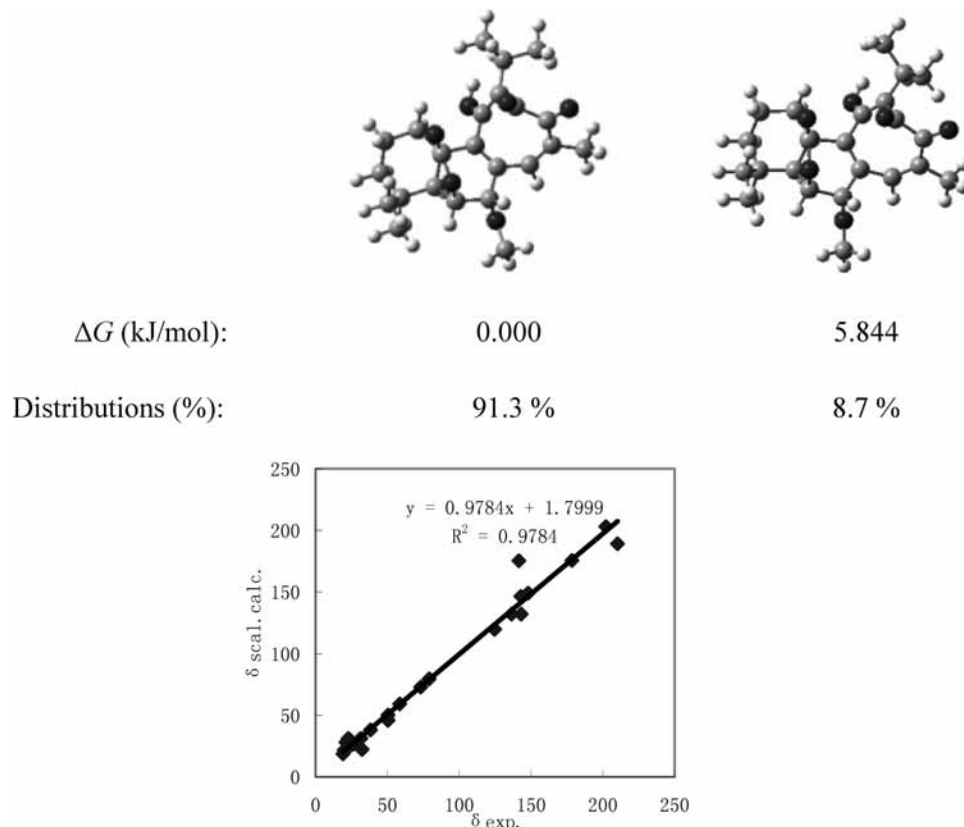


**Figure 3.** Structures and linear correlation between the scaled calculated (at the level of MPW1PW91/6-31G(d,p)-PCM//MPW1PW91/6-31G(d,p)) and experimental  $^{13}\text{C}$  NMR chemical shifts for **1**.

**TABLE 4: Differences between the Calculated<sup>a</sup> and Experimental  $^{13}\text{C}$  NMR Chemical Shifts for the Rightly Proposed Structure 2**

carbon no.	$\delta_{\text{calc.}}$	$\delta_{\text{scal. calc.}}$	$\delta_{\text{exp.}}^b$	$\Delta\delta_{(\text{calc.}-\text{exp.})}$	$\Delta\delta_{(\text{scal. calc.}-\text{exp.})}$
C-1	27.93	26.17	26.4	1.53	-0.23
C-2	20.74	18.79	18.6	2.14	0.19
C-3	38.16	36.67	38.14	0.02	-1.47
C-4	23.78	21.92	21.88	1.9	0.04
C-5	51.09	49.93	50.18	0.91	-0.25
C-6	74.93	74.39	73.02	1.91	1.37
C-7	79.90	79.48	79.45	0.45	0.03
C-8	132.36	133.30	132.07	0.29	1.23
C-9	150.15	151.55	146.62	3.53	4.93
C-10	50.09	48.90	45.83	4.26	3.07
C-11	185.32	187.63	189.11	-3.79	-1.48
C-12	119.97	120.59	119.82	0.15	0.77
C-13	172.25	174.22	175.41	-3.16	-1.19
C-14	145.19	146.46	149.08	-3.89	-2.62
C-15	133.97	135.96	132	1.97	2.96
C-16	35.39	33.82	30.2	5.19	3.62
C-17	20.50	18.55	22.76	-2.26	-4.21
C-18	57.52	56.53	59.19	-1.67	-2.66
C-19	200.02	202.71	203.12	-3.1	-0.41
C-20	30.60	28.91	28.08	2.52	0.83
C-21	23.05	21.17	22.34	0.71	-1.17
C-22	33.00	31.37	31.34	1.66	0.03
C-23	171.54	173.49	175.71	-4.17	-2.22
C-24	31.91	30.25	31.34	0.57	-1.09
				$ \Delta\delta _{\text{max}}$	4.93
				$ \Delta\delta _{\text{mean}}$	1.59

<sup>a</sup> The chemical shifts were computed at the MPW1PW91/6-31G(d,p) level of theory in the chloroform solvent, using the MPW1PW91/6-31G(d,p)-optimized geometries. <sup>b</sup> From ref 13a.

experiment values. Therefore, in the following discussions we only analyze the absorption spectra calculated by the TD-MPW1PW91/6-31G(d,p) method.

For przewalskin A (**3**), in the gas phase the calculated absorption wavelengths are 329.34, 277.78, and 250.91 nm, using the level of TD-MPW1PW91/6-31G(d,p). Compared with the absorption wavelengths in the gas phase, the absorption wavelengths in methanol solution are red-shifted. The differences between the calculated and experimental values are 1.89, 0.80, and 12.25 nm which means TD-MPW1PW91/6-31G(d,p)//MPW1PW91/6-31G(d,p) can predict accurately the adsorption spectra of przewalskin A (**3**). For przewalskin B (**4**), the calculated absorption wavelengths using the level of MPW1PW91/6-31G(d,p) are 331.50 and 256.19 nm in the gas phase. Solvent effect in methanol is considered by using the PCM model for przewalskin B (**4**), which makes the wavelengths change to 336.29 and 263.20 nm. In the methanol solvent the differences between the theoretical and experimental values are less than 6 nm.

The calculated absorption wavelengths of przewalskins A (**3**) and B (**4**) are in excellent agreement with experimental values. Therefore, UV-vis absorption spectra in the gas phase and solvents with use of DFT methods are predicted in order to correct the structure of hassananes (**1**).

For hassananes (**1**), the calculations in the gas phase give only one value of 240.36 nm whose oscillator strength is relatively large and the absorption wavelength 241.53 ppm in ethanol solvent is computed with the TD-MPW1PW91/6-31G(d,p)-PCM method. But the experimental absorption spectra have two peaks at 320 and 270 nm. The differences between the theoretical and the experimental absorption spectra are very large for hassananes (**1**). However, for compound **2** in the gas phase the absolute errors between the theoretical and experimental absorption spectra are 13.24 and 5.36 nm. In ethanol solvent, the absolute errors between the theoretical and experimental absorption spectra change to 16.42 and 6.21 nm. The

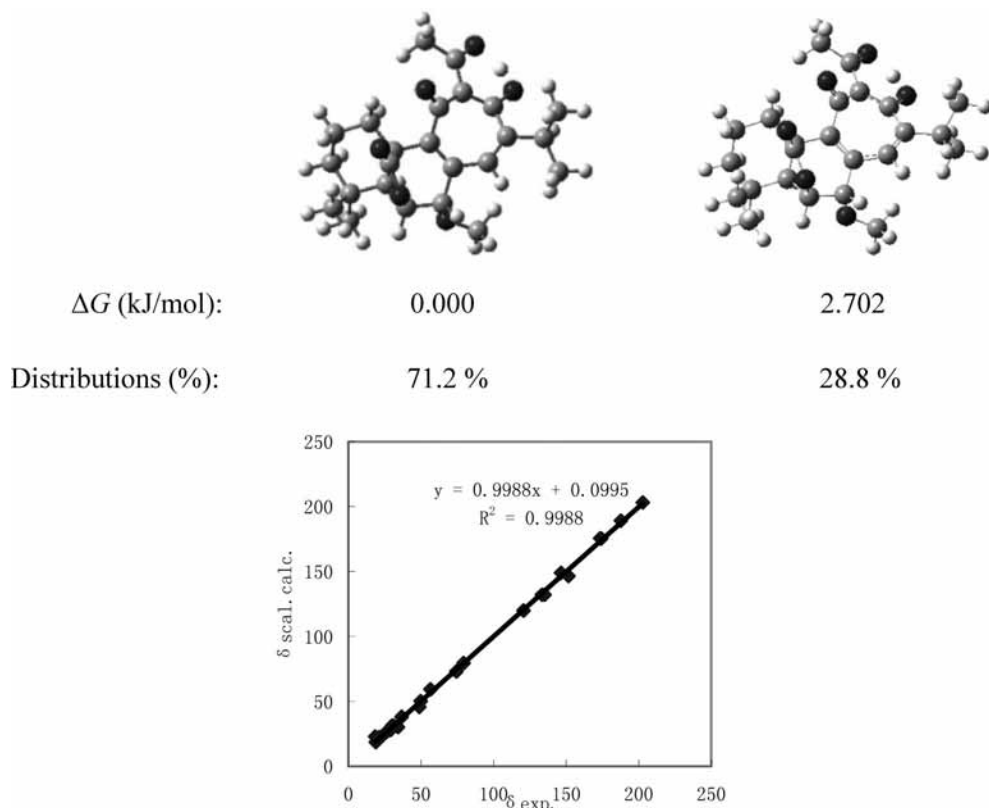


**Figure 4.** Structures and linear correlation between the scaled calculated (at the level of MPW1PW91/6-31G(d,p)-PCM//MPW1PW91/6-31G(d,p)) and experimental  $^{13}\text{C}$  NMR chemical shifts for **2**.

**TABLE 5: The Computed Absorption Wavelengths ( $\lambda_{\text{ad}}$ ) in Gas Phase and Solvent and Oscillator Strengths ( $f$ ) of Przewalskins A (**3**) and B (**4**) and the Experimental Values**

methods	species	<b>3</b>		<b>4</b>	
		$\lambda_{\text{ad}}/\text{nm}$	$f$	$\lambda_{\text{ad}}/\text{nm}$	$f$
TD-B3LYP/ 6-31G(d)	gas phase	341.35	0.064	341.59	0.103
		289.83	0.046	263.99	0.155
	261.99	0.076			
	methanol	336.45	0.109	346.45	0.138
		287.40	0.127	271.26	0.178
	261.98	0.100			
TD-MPW1PW91/ 6-31G(d,p)	gas phase	329.34	0.084	331.50	0.120
		277.78	0.064	256.19	0.180
	250.91	0.137			
	methanol	325.89	0.112	336.29	0.150
		276.80	0.145	263.20	0.212
	251.52	0.161			
exptl <sup>a</sup>	methanol	324	3.56 <sup>b</sup>	331	1.20 <sup>b</sup>
		276	2393.92 <sup>b</sup>	269	1.51 <sup>b</sup>
		1.20 <sup>b</sup>	3.82 <sup>b</sup>		

<sup>a</sup> From ref 14. <sup>b</sup> The values in italic denote log  $\epsilon$ .

differences of **2** between the theoretical and experimental absorption spectra are decreased largely compared with those of hassananes (**1**).

#### 4. Conclusions

In this work, MPW1PW91/6-31G(d,p)-optimized geometries followed by MPW1PW91/6-31G(d,p)  $^{13}\text{C}$  NMR chemical shift calculations in chloroform solvent are proposed here to be a good computational tool in the revision of the structure of natural product hassananes (**1**) by analyzing its  $^{13}\text{C}$  NMR spectra. Two compounds, przewalskins A (**3**) and B (**4**), were used to test the reliability of the computational method. The theoretical  $^{13}\text{C}$

**TABLE 6: The Computed Absorption Wavelengths ( $\lambda_{\text{ad}}$ ) in Gas Phase and Solvent and Oscillator Strengths ( $f$ ) of **1** and **2** and the Experimental Values**

methods	species	<b>1</b>		<b>2</b>	
		$\lambda_{\text{ad}}/\text{nm}$	$f$	$\lambda_{\text{ad}}/\text{nm}$	$f$
TD-B3LYP/ 6-31G(d)	gas phase	251.04	0.114	344.74	0.099
				255.87	0.148
	ethanol	251.58	0.109	342.09	0.072
TD-MPW1PW91/ 6-31G(d,p)	gas phase	240.36	0.107	333.24	0.116
				276.36	0.095
	ethanol	241.53	0.120	336.42	0.102
exptl <sup>a</sup>	ethanol			277.21	0.169
				320	320
				271	271

<sup>a</sup> From ref 13a.

NMR chemical shifts are determined by the Boltzmann averages of the GIAO  $^{13}\text{C}$  chemical shifts calculated for the two conformers of structures **1** and **2**. The least-squared parameters of linear correlation between experimental and theoretical  $^{13}\text{C}$  NMR chemical shifts allowed reassigning the considered structure **1** to **2**. Furthermore, we investigated the absorption spectra of przewalskins A (**3**) and B (**4**) as well as structures **1** and **2** using TD-DFT methods and the solvent effect is taken into account by using PCM model. Through analyzing the match between the calculated and experimental absorption spectra in ethanol solvent, it is validated again that the proposed structure **2** is right.

**Acknowledgment.** Financial support for this research was provided by The National Basic Research Program (973 program; no. 2009 CB 522300).

## References and Notes

- (1) Barone, G.; Paloma, L. G.; Duca, D.; Silvestri, A.; Riccio, R.; Bifulco, G. *Chem. Eur. J.* **2002**, *8*, 3233.
- (2) Rychnovsky, S. D. *Org. Lett.* **2006**, *8*, 2895.
- (3) Aberle, N.; Ovenden, S. P. B.; Lessene, G.; Watsona, K. G.; Smith, B. J. *Tetrahedron Lett.* **2007**, *48*, 2199.
- (4) Braddock, D. C.; Rzepa, H. S. *J. Nat. Prod.* **2008**, *71*, 728.
- (5) Sebag, A. B.; Forsyth, D. A.; Plante, M. A. *J. Org. Chem.* **2001**, *66*, 7967.
- (6) Barone, G.; Duca, D.; Silvestri, A.; Paloma, L. G.; Riccio, R.; Bifulco, G. *Chem. Eur. J.* **2002**, *8*, 3240.
- (7) Stephens, P. J.; Pan, J. J.; Devlin, F. J.; Krohn, K.; Kurtán, T. *J. Org. Chem.* **2007**, *72*, 3521.
- (8) Bringmann, G.; Mühlbacher, J.; Reichert, M.; Dreyer, M.; Kolz, J.; Speicher, A. *J. Am. Chem. Soc.* **2004**, *126*, 9283.
- (9) Guillaume, M.; Champagne, B.; Zutterman, F. *J. Phys. Chem. A* **2006**, *110*, 13007.
- (10) Manoj, N.; Ajayakumar, G.; Gopidas, K. R.; Suresh, C. H. *J. Phys. Chem. A* **2006**, *110*, 11338.
- (11) Jacquemin, D.; Perpète, E. A.; Assfeld, X.; Scalmani, G.; Frisch, M. J.; Adamo, C. *Chem. Phys. Lett.* **2007**, *438*, 208.
- (12) Ren, A. M.; Goddard, J. D. *J. Photochem. Photobiol. B* **2005**, *81*, 163.
- (13) (a) Luis, J. G.; Lahlou, E. H.; Andrés, L. S. *Tetrahedron* **1996**, *52*, 12309. (b) Luis, J. G.; Lahlou, E. H.; San Andrés, L.; Sood, G. H. N.; Ripoll, M. M. *Tetrahedron Lett.* **1996**, *37*, 4213.
- (14) Xu, G.; Hou, A. J.; Wang, R. R.; Liang, G. Y.; Zheng, Y. T.; Liu, Z. Y.; Li, X. L.; Zhao, Y.; Huang, S. X.; Peng, L. Y.; Zhao, Q. S. *Org. Lett.* **2006**, *8*, 4453.
- (15) Becke, A. D. *J. Chem. Phys.* **1993**, *98*, 5648.
- (16) Adamo, C.; Barone, V. *J. Chem. Phys.* **1998**, *108*, 664.
- (17) Ditchfield, R. *Mol. Phys.* **1974**, *27*, 789.
- (18) Rohlfing, C. M.; Allen, L. C.; Ditchfield, R. *Chem. Phys.* **1984**, *87*, 9.
- (19) Wolinski, K.; Hinton, J. F.; Pulay, P. *J. Am. Chem. Soc.* **1990**, *112*, 8251.
- (20) Miertus, S.; Scrocc, E.; Tomasi, J. *J. Chem. Phys.* **1981**, *55*, 117.
- (21) Miertus, S.; Tomasi, J. *J. Chem. Phys.* **1982**, *65*, 239.
- (22) Cossi, M.; Barone, V.; Cammi, R.; Tomasi, J. *Chem. Phys. Lett.* **1996**, *255*, 327.
- (23) Ditchfield, R. *Mol. Phys.* **1974**, *27*, 789.
- (24) Rohlfing, C. M.; Allen, L. C.; Ditchfield, R. *Chem. Phys.* **1984**, *87*, 9.
- (25) Wolinski, K.; Hinton, J. F.; Pulay, P. *J. Am. Chem. Soc.* **1990**, *112*, 8251.
- (26) Bauernschmitt, R.; Ahlrichs, R. *Chem. Phys. Lett.* **1996**, *256*, 454.
- (27) Casida, M. E.; Jamorski, C.; Casida, K. C.; Salahub, D. R. *J. Chem. Phys.* **1998**, *108*, 4439.
- (28) Jamorski, C.; Casida, M. E.; Salahub, D. R. *J. Chem. Phys.* **1996**, *104*, 5134.
- (29) Stratmann, R. E.; Scuseria, G. E.; Frisch, M. J. *J. Chem. Phys.* **1998**, *109*, 8218.
- (30) Frisch, M. J.; Trucks, G. W.; Schlegel, H. B.; Scuseria, G. E.; Robb, M. A.; Cheeseman, J. R.; Montgomery, J. A., Jr.; Vreven, T.; Kudin, K. N.; Burant, J. C.; Millam, J. M.; Iyengar, S. S.; Tomasi, J.; Barone, V.; Mennucci, B.; Cossi, M.; Scalmani, G.; Rega, N.; Petersson, G. A.; Nakatsuji, H.; Hada, M.; Ehara, M.; Toyota, K.; Fukuda, R.; Hasegawa, J.; Ishida, M.; Nakajima, T.; Honda, Y.; Kitao, O.; Nakai, H.; Klene, M.; Li, X.; Knox, J. E.; Hratchian, H. P.; Cross, J. B.; Bakken, V.; Adamo, C.; Jaramillo, J.; Gomperts, R.; Stratmann, R. E.; Yazyev, O.; Austin, A. J.; Cammi, R.; Pomelli, C.; Ochterski, J. W.; Ayala, P. Y.; Morokuma, K.; Voth, G. A.; Salvador, P.; Dannenberg, J. J.; Zakrzewski, V. G.; Dapprich, S.; Daniels, A. D.; Strain, M. C.; Farkas, O.; Malick, D. K.; Rabuck, A. D.; Raghavachari, K.; Foresman, J. B.; Ortiz, J. V.; Cui, Q.; Baboul, A. G.; Clifford, S.; Cioslowski, J.; Stefanov, B. B.; Liu, G.; Liashenko, A.; Piskorz, P.; Komaromi, I.; Martin, R. L.; Fox, D. J.; Keith, T.; Al-Laham, M. A.; Peng, C. Y.; Nanayakkara, A.; Challacombe, M.; Gill, P. M. W.; Johnson, B.; Chen, W.; Wong, M. W.; Gonzalez, C.; Pople, J. A. *Gaussian 03*, revision C.02; Gaussian, Inc.: Wallingford, CT, 2004.

JP8072415